Volume 6 | Number 47 | 21 December 2018 | Pages 7763–8000

Journal of Materials Chemistry B

Materials for biology and medicine

rsc.li/materials-b

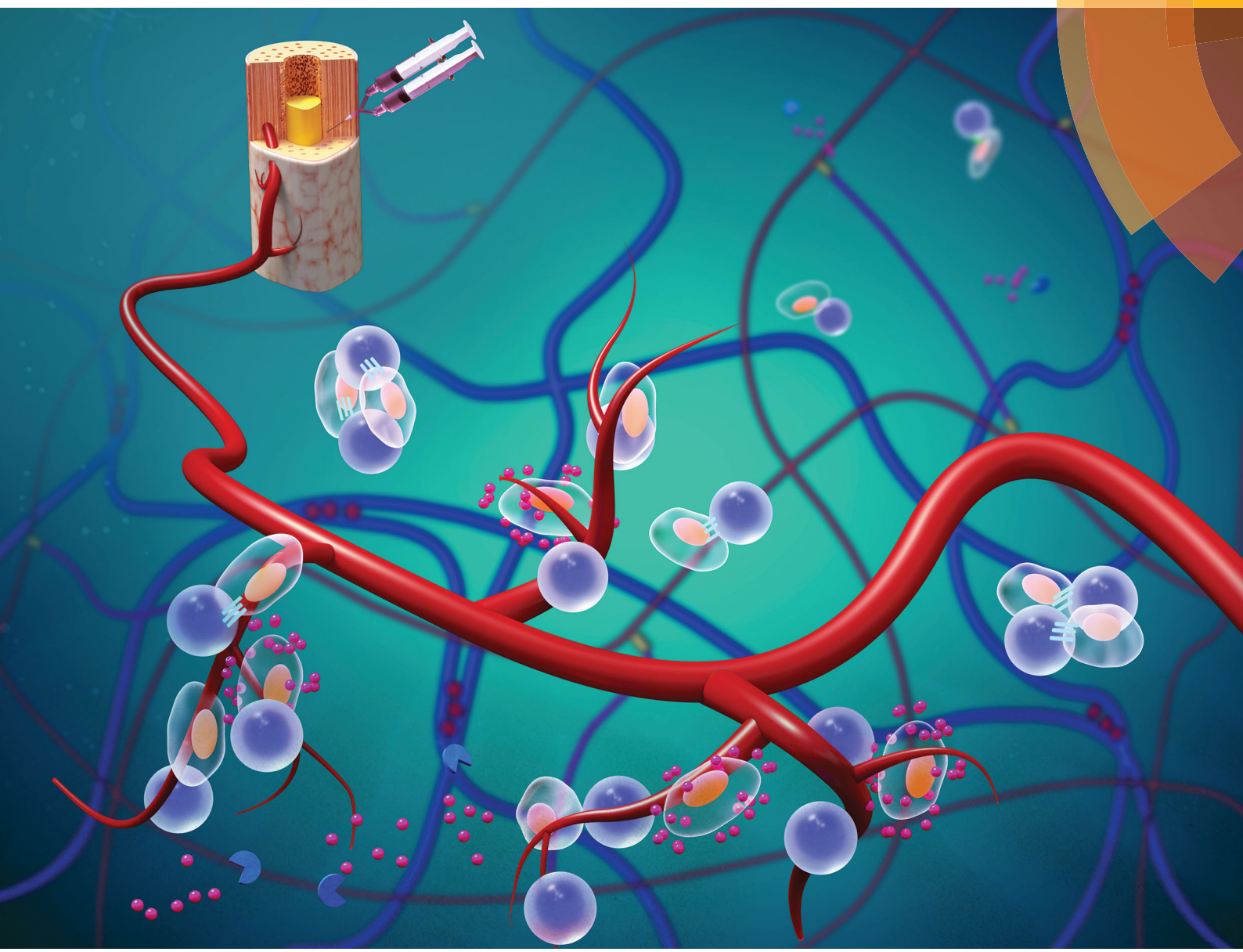

ISSN 2050-750X

ROYAL SOCIETY OF CHEMISTRY

PAPER

Xiaozhong Qu, Xiaoyan Wang *et al.*

An injectable double-network hydrogel for the co-culture of vascular endothelial cells and bone marrow mesenchymal stem cells for simultaneously enhancing vascularization and osteogenesis

Journal of Materials Chemistry B

PAPER

View Article Online
View Journal | View Issue

Cite this: J. Mater. Chem. B, 2018, 6, 7811

An injectable double-network hydrogel for the co-culture of vascular endothelial cells and bone marrow mesenchymal stem cells for simultaneously enhancing vascularization and osteogenesis†

Congchong Yang,[a] Bing Han,[a] Chunling Cao,[a] Di Yang,[b] Xiaozhong Qu *[b] and Xiaoyan Wang *[a]

Received 25th August 2018,
Accepted 4th October 2018

DOI: 10.1039/c8tb02244e

rsc.li/materials-b

The achievement of rapid vascularization in large implanted constructs is a major challenge in the field of bone tissue engineering. Although co-culture of bone-forming cells and vascular endothelial cells (VECs) has been expected to be a way of promoting vascularization during bone formation with a scaffold, there is a lack of detailed knowledge about the direct interactions between two types of stem cells in a three-dimensional (3D) extracellular matrix (ECM). Herein, we report on the use of an injectable cytocompatible double-network (DN) hydrogel to encapsulate, co-culture and subsequently stimulate the angiogenic/osteogenic differentiation of VECs and the human bone marrow mesenchymal stem cells (BM-MSCs), which demonstrates that the direct co-cultured system enables simultaneous enhancement of vascularization and osteogenesis by providing 3D cell–cell communication. Besides, the improved mechanical properties and the injectability of the DN hydrogel allow the delivery, long-time implantation, proliferation and differentiation of stem cells *in vivo*. Therefore, this study could provide a niche-like native ECM for stem cell survival and the regulation of the differentiation of multiple cell lines which will benefit bone repair.

1. Introduction

For bone tissue engineering, vascularization remains one of the main obstacles that must be overcome to reconstruct large bone defects. The development of rapid vascularization after implantation could supply the growing osteoblast cells with the nutrients to grow and survive.[1,2] In recent years, extensive research has been dedicated to improving the vascularization of a tissue-engineered construct.[3] These strategies include improved scaffold design by enhancing pore size and interconnectivity,[4] addition of specific proangiogenic factors,[5] as well as co-cultures of bone-forming cells and vascular endothelial cells (VECs) into a biomaterial composite to repair bone defects.[6,7] In recent studies, biomaterials have been designed for promoting the rate of bone formation and vascularization by enhancing the two cell contacts and secretion of angiogenic factors within these co-cultures.[8,9]

Importantly, it has been reported that the effects of biomaterials on a single type of cell are different from that on co-culture systems, which mimic much better the real situation of tissue regeneration in which different types of cells are involved.[10,11] The cells regard each other as their surrounding microenvironment, and thus the biomechanical or biochemical cues from neighboring cells represent a way of stimulating angiogenic and osteogenic differentiation.[7] It is necessary to have a better understanding of the biological processes underlying vascularization/osteogenesis and cell–cell communication between VECs and bone-forming cells. However, detailed knowledge about their direct interactions with each other in three-dimensional (3D) biomaterial scaffolds remains limited.

Biomaterial-based 3D structures provide an ideal platform for cell–cell and cell–material communications and induce cells to behave in a manner that is a step closer to the natural conditions.[12,13] A multifunctional 3D model of stem-cell niche would allow stem cells embedding in an artificial microenvironment that more closely mimics the natural extracellular matrix

[a] Department of Cariology and Endodontology, National Engineering Laboratory for Digital and Material Technology of Stomatology, Peking Key Laboratory of Digital Stomatology, Peking University School and Hospital of Stomatology, Beijing 100081, China. E-mail: wangxiaoyan@pkuss.bjmu.edu.cn
[b] College of Materials Science and Opto-electronic Technology, University of Chinese Academy of Sciences, Beijing 100049, China. E-mail: quxz@iccas.ac.cn

† Electronic supplementary information (ESI) available. See DOI: 10.1039/c8tb02244e

(ECM) deliver diffusible cytokines to promote tissue-specific differentiation and manipulation at a desired time during an experiment.[14] Applications of hydrogels suggested that the construction of such complex 3D microenvironments would be possible and could allow scaffold-based culture systems to study stem cell biology under more realistic conditions.[15,16] In our previous study, we combined two kinds of dynamic interactions, *i.e.* dynamic covalent bonding with ionic interaction, to make an *in situ* forming and injectable double-network (DN) hydrogel based on glycol chitosan (GC) and calcium alginate (Alg). The sol–gel transition was achieved under very mild conditions without the inclusion of any external stimuli or toxic initiator, and producing only NaCl and water, which was proven to be an excellent matrix for the loading and *in vitro* proliferation of living cells.[17] Besides, the DN hydrogel showed enhanced mechanical properties and lower degradation kinetics when compared to the parent individual network hydrogels. More importantly, owing to the reversibility of the crosslinks, we expect that the hydrogel is more favorable for the stereoscopic cell-to-cell connection during the proliferation than the permanently crosslinked hydrogels. It is known that the microenvironment of the ECM, *e.g.* the chemical structure and mechanical strength of hydrogels, would affect the cell behaviors, for example, seriously influencing the way of stem cell differentiation. Compared to cell adhesive surfaces, an *in situ* forming hydrogel provides 3D space and a more hydrophilic microenvironment for the distribution and growth of cells and furthermore may regulate cellular physiological functions *via* a mechanotransduction pathway. Therefore, the cytocompatible GC/Alg DN hydrogel should be an ideal platform for stimulation and subsequent investigation of long-term (*e.g.* a few weeks) cell performances in a 3D matrix.

Herein, we utilize the GC/Alg DN hydrogel to simultaneously incorporate VECs and human bone marrow mesenchymal stem cells (BM-MSCs) in order to reveal the effect of direct cell–cell communication on enhancing vascularization and osteogenesis *in vitro* and *in vivo*. We suppose that the co-culture of BM-MSCs with VECs in 3D will promote angiogenic and osteogenic differentiation of stem cells simultaneously (Scheme 1). If so, the GC/Alg DN hydrogel may provide a new option for vascularized bone regeneration, with injectability as well as desirable mechanical properties.

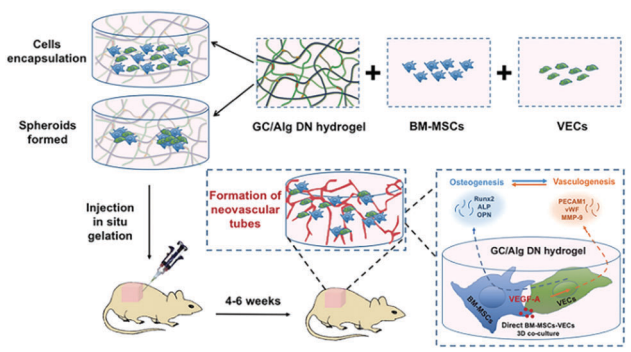

Scheme 1 Preparation and utilization of a GC/Alg DN hydrogel as a 3D scaffold for the co-culture of BM-MSCs with VECs to promote vascularization and osteogenesis simultaneously.

2. Experimental

2.1. Materials

Poly(ethylene oxide) (PEO, MW = 2 kDa), glycol chitosan (GC, MW ~ 250 kDa), and sodium alginate (MW ~ 150 kDa, M/G ratio ~ 1.6) were purchased from Sigma-Aldrich (St. Louis, USA). Benzaldehyde-capped poly(ethylene oxide) (OHC-PEO-CHO) was synthesized according to our previous report.[18,19] Dulbecco's Modified Eagle's Medium (DMEM), 0.25% trypsin-EDTA, penicillin–streptomycin solution, and phosphate-buffered saline (PBS) were purchased from Gibco (Grant Island, USA). Mesenchymal Stem Cell Medium (MSCM) and fetal bovine serum (FBS) were purchased from ScienCell (San Diego CA, USA). A Live/Dead cell imaging kit was purchased from Invitrogen (Eugene, OR, USA). Organic solvents and other compounds were all obtained from Beijing Chemical Reagents Company (China).

2.2. Formation of GC, Alg and GC/Alg double-network (DN) hydrogels

The GC/OHC-PEO-CHO (GC gel) was achieved by mixing aqueous solutions containing 4% w/v GC and 1% w/v OHC-PEO-CHO, calcium alginate (Alg gel) was achieved by mixing aqueous solutions containing 2% w/v sodium alginate (Alg) and 1% w/v calcium chloride ($CaCl_2$). The constituent solutions were added in a mold and then kept still for 30 min at room temperature to allow gelation. The typical method for preparing the double-network hydrogel (GC/Alg DN gel) was first to prepare two aqueous solutions containing GC and $CaCl_2$, and OHC-PEO-CHO and Alg, respectively, at calculated concentrations as GC and Alg gels, and an equal volume of the solutions was added in a mold, mixed, under violent stirring for 1 min, and then made to stand still for 30 min at room temperature to allow gelation. For injectable samples, the solutions of GC and $CaCl_2$, and Alg and OHC-PEO-CHO were made at designed concentrations as above. The solutions were loaded into two 2.5 ml syringes at equal volume which were then mounted to a connected mixing syringe for an injection.

2.3. Characterization of GC, Alg and GC/Alg double-network (DN) hydrogels

Mechanical tests. Mechanical property tests were performed using an INSTRON 3367 machine (Norwood, MA, USA) at room temperature in air. For the compressive property test, the samples were molded in a cylinder shape of 10 mm in diameter (d) and 10 mm in height (h). The rate of compression was fixed at 100 N and 1 mm min^{-1} with a maximum compressive strain set at 90%. The experiments were conducted in triplicate.

Scanning electron microscopy (SEM) analysis. The morphology of hydrogels was observed using SEM (S-4800, Hitachi, Japan). The samples were prepared by the freeze-fracture method through immersing the hydrogel into liquid nitrogen, freeze dried, sliced up and sputter coated with gold for SEM observation. For the observation of morphological structure of the cells encapsulated in the GC/Alg DN hydrogel, the gel was fixed in 2.5% glutaradehyde for 2 h, immersed in 0.18 mol L^{-1} sucrose at 4 °C for 2 h, rehydrated in ethanol series, and then prepared as the freeze-fracture method above.

***In vitro* degradation studies.** *In vitro* degradation of the hydrogels was examined according to weight loss with time up to 4 weeks. The GC gel, Alg gel and GC/Alg DN gel (0.2 ml) were weighed and then immersed in 2 ml water at room temperature, respectively. The weight loss of hydrogels was monitored as a function of incubation time by replacing the incubation solution with an equal volume of water at a specified time interval. The incubation solutions collected at each time point were lyophilized and weighed. The experiments were conducted in triplicate.

2.4. Cell culture and cytotoxicity assay

Cell culture. Human vascular endothelial cells (EA.hy926) were obtained from Shanghai cell bank of the Chinese Academy of Sciences. The cells were maintained in DMEM, (Invitrogen) supplemented with 10% FBS (ScienCell), and penicillin (100 U ml^{-1})/streptomycin (100 μg ml^{-1}) (Invitrogen). Human Bone Marrow-derived Mesenchymal Stem Cells (BM-MSCs) were obtained from ScienCell Research Laboratories. The cells were maintained in MSCM (ScienCell) supplemented with 5% FBS (ScienCell) and Mesenchymal Stem Cell Growth Supplement (MSCGS, ScienCell) and penicillin (100 U ml^{-1})/streptomycin (100 μg ml^{-1}) (ScienCell). The cells were maintained at 37 °C in a 5% CO_2, 95% humidified atmosphere.

Cytotoxicity assay. The GC, Alg and DN hydrogels (0.2 ml) were immersed in 2 ml DMEM and MSCM at 37 °C for 72 h, respectively. The leach liquors were collected to deal with EA.hy926 or BM-MSCs. The cell counting kit-8 (CCK-8) assay was performed to assess the cytotoxicity of gels. The cells were plated in 96-well plates (Corning) at an initial density of 2×10^3 cells per well, synchronized with serum-free medium for 24 h, and then the culture medium was removed by the leach liquors of gels for incubation at 37 °C for 24 h and 48 h. Then the cells were treated with 10% CCK-8 reagent medium solution and incubated at 37 °C for 2 h. The absorbance of samples in triplicate wells was measured with an automatic enzyme-linked immunosorbent assay reader (ELx800, BioTek Instruments, Inc., USA) at a wavelength of 450 nm.

2.5. *In vitro* 3D cell culture and cell proliferation in the GC/Alg DN hydrogel

***In vitro* 3D cell culture.** For *in vitro* experiments, two solutions containing GC (4% w/v) and $CaCl_2$ (1% w/v), and Alg (2% w/v) and OHC-PEO-CHO (1% w/v) were prepared respectively. EA.hy926 (2×10^5 ml^{-1}) suspended in DMEM and BM-MSCs (2×10^5 ml^{-1}) suspended in MSCM were added to OHC-PEO-CHO solution respectively. The GC/$CaCl_2$ and Alg/OHC-PEO-CHO solutions were then mixed together and injected into 96-well plates to achieve sol–gel transition. The DN hydrogels loaded with EA.hy926 or BM-MSCs or co-cultured EA.hy926 and BM-MSCs (1 : 1, 2×10^5 ml^{-1}) were then cultured at 37 °C, 5% CO_2.

Cell proliferation assay. The cell proliferation ability was detected by CCK-8 and Live/Dead assay. The CCK-8 assay was performed at expected time within 3 weeks (0 d, 4 d, 7 d, 14 d, and 21 d) as the method above. After incubation for predetermined time, the hydrogels were stained by Live Green and Dead Red reagents for 15 min at 25 °C. The samples were cut into slices and transferred to a fluorescence microscope for observation.

2.6. Angiogenic/osteogenic differentiation of VECs and BM-MSCs in the GC/Alg DN hydrogel

Gene expression assay. The GC/Alg DN hydrogel loaded with cells for *in vitro* culture was prepared as above. Total RNA was extracted from the cells using the TRIzol reagent (Invitrogen). For cDNA synthesis, mRNA was reverse-transcribed into cDNA using the 5× PrimeScript RT Master Mix (TaKaRa) at 37 °C for 15 min and 85 °C for 5 s according to the manufacturer's protocol. The synthesized cDNA samples were subjected to determine the expression of VEGF-A, PECAM1, vWF, MMP-9, Runx2, ALP, OPN, OCN and Col Iα1. Gene expression was quantified by Real-Time Quantitative PCR using SYBR Green master rox (Roche Diagnostics Ltd, Mannheim, Germany) with a 7500 ABI Real-Time PCR System (Applied Biosystems, Foster City, CA, USA). The relative gene expression was calculated using the $2(-\Delta\Delta CT)$ method. Briefly, the resultant mRNA was normalized to its own GAPDH. The following primers were utilized for the Real-Time RT-PCR. GAPDH (5′-GAAGGTG AAGGTCGGAGTC-3′, 5′-GAGATGGTGATGGGAT TTC-3′), VEGF-A (5′-TCACAGGTACAGGGATGAGGACAC-3′, 5′-CAAAG CACAGCA ATGTCCTGAAG-3′), PECAM1 (5′-CCTCCAGCCCTAGAAGCCA ATTA-3′, 5′-CTCAAAGACTGAGTCAGGCCAGTG-3′), vWF (5′-TG AACAC AAGTGTCTGGCTGAGG-3′, 5′-CAGTGATGTCGTTGCA CTCAGG-3′), MMP-9 (5′-ACGCACGACGTCTTCCAGTA-3′, 5′-CC ACCTGGTTCAACTCA CTCC-3′), Runx2 (5′-TCACCTCAGGCATG TCCCTCGGTAT-3′, 5′-TGGCT TCCATCAGCGTCAACACC-3′), ALP (5′-GAGTCGGACGTGTACCGGA-3′, 5′-TGCCACTCCCACA TTTGTCAC-3′), OPN (5′-ATGGAAAGCGAGGAGTT GAATG-3′, 5′-TGCTTGTGGCTGTGGGTTT-3′), OCN (5′-CACTCCTCGCCC TATTGGC-3′, 5′-CCCTCCTGCTTGGACACAAAG-3′), and Col Iα1 (5′-TAGGGTCTAGACATGTTCAGCTTTG-3′, 5′-CGTTCTGTACGC AGGTGATT G-3′).

Immunofluorescence assay. For immunofluorescence assay, the DN hydrogel encapsulated with cells was fixed in 4% paraformaldehyde (PFA) for 20 min at room temperature, permeabilized with 1% Triton X-100 for 15 min and blocked with goat serum albumin for 30 min at 37 °C, followed by an overnight incubation at 4 °C with antibodies specific for CD31 (1 : 20, Abcam, Cambridge MA, USA) or RUNX2 (1 : 100, Abcam). The appropriate secondary antibodies (diluted 1 : 50) were then used, and then nuclei were stained by 4,6-diamidino-2-phenylindole (DAPI, 1 : 1000, Invitrogen) for 2 min. Immunofluorescence was visualized using a Zeiss LSM-710 laser-scanning confocal microscope (LSCM).

Von Kossa staining. The 4% PFA-fixed, paraffin-embedded specimens were cut at 4 μm interval, heated for 3 h at 60 °C, deparaffinized in xylene, and rehydrated in ethanol series. The sections were incubated in 5% silver nitrate solution for 1 h under ultraviolet light, and then incubated in 0.1% nuclear solid red dye for 10 min.

2.7. *In vivo* animal experiments

Subcutaneous injection of GC/Alg DN hydrogels in nude mice. Male BALB/c mice (5–6 weeks of age, 20 ± 2 g) were

purchased from Beijing Vital River Laboratory Animal Technology Co., Ltd (China). All animal experiments were performed in compliance with the relevant laws and institutional guidelines of Peking University and approved by the Experimental Animal Welfare Ethics Section of Peking University Biomedical Ethics Committee (approval number: LA2017049). For *in vivo* experiments, two solutions containing GC (4% w/v) and $CaCl_2$ (1% w/v), and Alg (2% w/v) and OHC-PEO-CHO (1% w/v) were prepared respectively. EA.hy926 (2×10^5 ml^{-1}) suspended in serum-free DMEM and BM-MSCs (2×10^5 ml^{-1}) suspended in serum-free MSCM were added to the OHC-PEO-CHO solution respectively. The GC/$CaCl_2$ and Alg/OHC-PEO-CHO solutions were then loaded into syringes and mounted into a connected mixing syringe for injection. A total of 36 nude mice were involved in the test, which were divided into 4 groups including the GC/Alg DN hydrogel (DN), GC/Alg DN hydrogel loaded with VECs (DN-EC), GC/Alg DN hydrogel loaded with BM-MSCs (DN-BM), and GC/Alg DN hydrogel loaded with VECs and BM-MSCs (DN-EC-BM). A 0.4 ml aliquot of gel solution was injected subcutaneously into the left and right sides of the dorsal region of each nude mouse at room temperature. At 2, 4, and 6 weeks post-injection, 12 animals were sacrificed and the dorsal skin around the implantation site was carefully incised to isolate the skin tissue with the residue of the gel implants (6 samples of each group). The tissues were immediately fixed in 10% formaldehyde for histopathological characterization.

Histological analysis. For immunohistochemical (IHC) analysis, the formalin-fixed, paraffin-embedded specimens were cut at 4 μm interval, heated for 3 h at 60 °C, deparaffinized in xylene, and rehydrated in ethanol series. Antigen was retrieved with microwave heating in citrate retrieval buffer (pH 6.0) for 20 min, and then washed three times with PBS for 5 min. Endogenous peroxidase activity was blocked with 3% hydrogen peroxide for 15 min at room temperature followed by washing with PBS plus 0.1% Tween 20. The slides were incubated with a primary monoclonal anti-human CD31 (1 : 50, Abcam) antibody at 4 °C overnight. After washing with PBS buffer, the sections were incubated with the streptavidin-conjugated horseradish peroxidase (HRP) (MaxVision, Fuzhou, China) for 15 min. Finally, the reaction complexes were viewed using a diaminobenzidine kit (Maixin Biotechnology, Fuzhou, China). PBS was used in all negative controls of IHC.

2.8. Statistical analysis

The data were representative of three or more independent experiments as the mean ± standard deviation (SD). Statistical significance was assessed using one-way analysis of variance (ANOVA) and Student's unpaired *t*-test, using the SPSS 25.0 software package. *P*-Value <0.05 was considered significant.

3. Results and discussion

3.1. Preparation and characterization of a GC/Alg double-network (DN) hydrogel

Four components were involved in the construction of a DN gel, that is, glycol chitosan (GC), dibenzaldehyde functionalized poly(ethylene oxide) (OHC-PEO-CHO), sodium alginate (Alg), and calcium chloride ($CaCl_2$). The GC/$CaCl_2$ and Alg/OHC-PEO-CHO solutions were mixed together and injected into 96-well plates to achieve sol–gel transition (Fig. 1A). With the given components, the gelation time of the GC/Alg DN hydrogel was 80 s. According to our previous work, in the resultant DN hydrogel, GC and OHC-PEO-CHO formed a benzoic–imine bond by Schiff's reaction to generate the first network, while Alg and $CaCl_2$ formed supramolecular ionic interaction to generate the second network.[17]

The injectable property is demonstrated in Fig. 1B, and it could be seen that the injection was easily performed using a

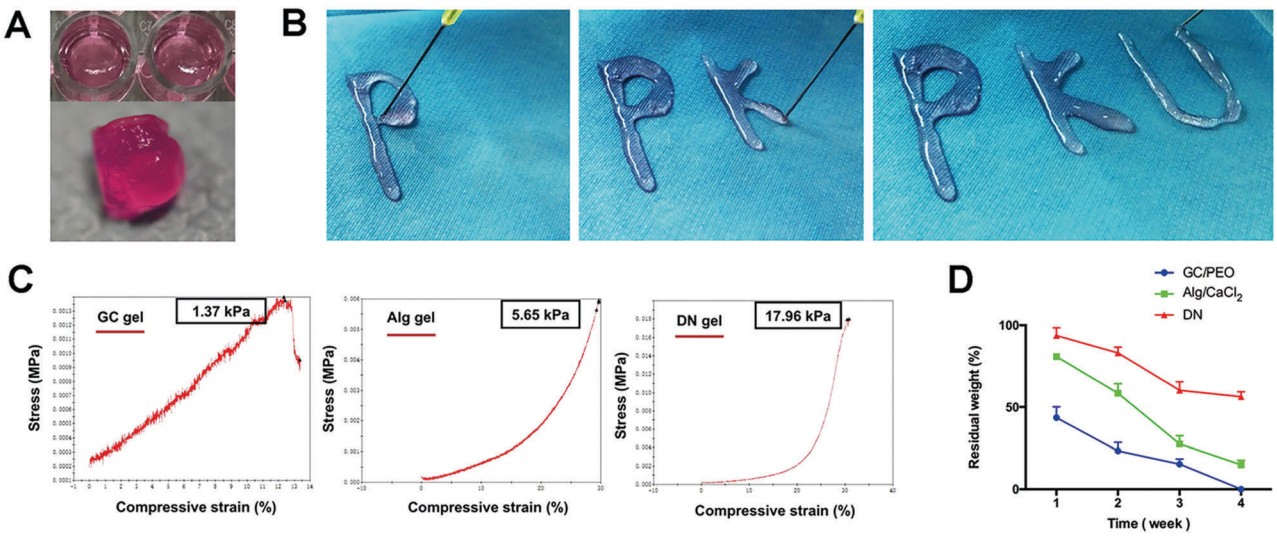

Fig. 1 Preparation and characterization of GC/Alg double-network (DN) hydrogel. (A) The GC/Alg DN hydrogel (containing 4% w/v GC, 1% w/v OHC-PEO-CHO, 2% w/v sodium alginate, and 1% w/v $CaCl_2$, respectively) was injected into the 96-well plates to achieve sol–gel transition and formed complete cylinder shape. (B) Demonstration of the injectability of the GC/Alg DN hydrogel through a connected mixing syringe of 24 G needle. (C) Compressive stress–strain curve showing the compressive resistance failure point of GC, Alg, and GC/Alg DN hydrogels. (D) *In vitro* degradation curves showing the residual weight of GC, Alg, and GC/Alg DN hydrogels within 4 weeks. The bar represents the mean ± SD.

connected mixing syringe and the DN hydrogel was formed by gelation sooner after the polymer solutions were extruded out of the syringe needle. The injective property of the sol–gel transition of the DN gel was mainly driven by the network which had the relative faster gelation kinetics. The porous structure in the freeze-dried DN gel was demonstrated by scanning electron microscopy (SEM) (Fig. S1, ESI†). Under compressive loading, it can be seen that the GC gel exhibited a brittle rupture, the Alg gel exhibited unrecoverable ductile failure, and the DN gel exhibited suitably elastic resilience (Fig. S2, ESI†). The compressive stress–strain curve showed that the compressive resistance failure point of the DN gel was 17.96 kPa, while it was only 1.37 kPa and 5.65 kPa for the GC gel and Alg gel (Fig. 1C). The results of mechanical characteristics indicated that the DN hydrogel harvested significantly higher compressive strength than the parent single-network GC and Alg gels. The combination of the two single networks resulted in a condensed polymer network, stronger interaction, and more entanglements in the DN gels and thus led to an increase of the elastic modulus. Within the experimental duration of 4 weeks, the degradation of the gels *in vitro* was tested. As shown in Fig. 1D, the GC/Alg DN hydrogel exhibited 60.27% residual weight at 3 weeks, while it was 27.51% and 15.26% for the parent Alg and GC gels. Up to 4 weeks, the GC gel was completely degraded, the Alg gel had only 14.89% weight left, however the GC/Alg DN hydrogel was monitored to maintain 56.33% residual weight. This result revealed that the GC/Alg DN gel exhibited a much slower degradation rate than the parent GC and Alg gels. Due to the more compact networks, DN reduced the diffusion rate of the polymer chains in case the crosslink points were broken by solvent molecules, and hence the chains would be able to re-crosslink owing to the reversibility of imine-bonding or calcium complexation.

3.2. Survival and proliferation of VECs and BM-MSCs encapsulated in the GC/Alg DN hydrogel

The CCK-8 assay was performed to detect the cytotoxicity of the gels *in vitro*. EA.hy926 and BM-MSCs cultured in the leach liquor of GC, Alg and DN gels for 24 h and 48 h reached a cell viability of higher than 90% compared with that in a complete cell culture medium (DMEM for EA.hy926 and MSCM for BM-MSCs), which indicated that the GC, Alg and DN gels have no cytotoxicity (Fig. 2A and B).

To more thoroughly explore GC/Alg DN hydrogel's potential of serving as a biomimetic ECM scaffold for vascularization and bone repair, we encapsulated VECs and BM-MSCs into the DN hydrogel by mixing cells with OHC-PEO-CHO solution prior to sol–gel transition of the DN hydrogel, respectively. The cell-loaded DN hydrogel was subjected to an *in vitro* cell culture up to 21 days. As shown in Fig. 2C, the EA.hy926 and BM-MSCs encapsulated in the GC/Alg DN hydrogel exhibited round shape and the cells were uniformly distributed in the 3D gel matrix under an inverted phase-contrast microscope. The same morphology of EA.hy926 and BM-MSCs in the formed DN hydrogel can also be observed under SEM. As shown in SEM images both EA.hy926 and BM-MSCs presented good cell viability in the porous structure of DN gels, and orbicular cell division could be observed (marked with an arrow) (Fig. 2C).

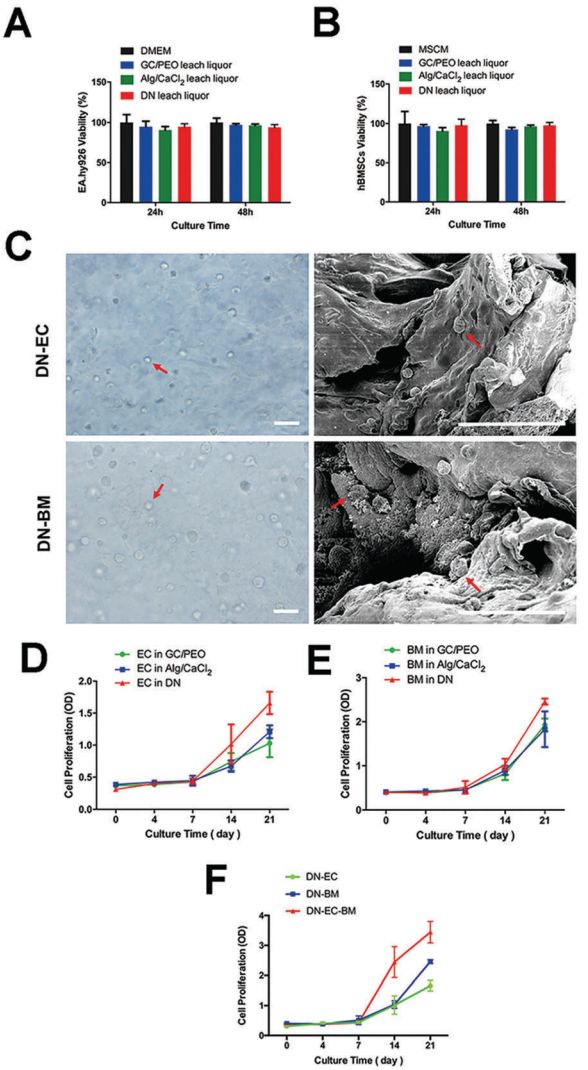

Fig. 2 Survival and proliferation of VECs and BM-MSCs encapsulated in the GC/Alg DN hydrogel. (A and B) The CCK-8 assay revealed that GC, Alg, and GC/Alg DN hydrogels have no cytotoxicity for the cell culture of VECs and BM-MSCs. (C) The VECs and BM-MSCs encapsulated in the GC/Alg DN hydrogel exhibited round shape and the cells were uniformly distributed in the 3D gel matrix. The images were captured under an inverted microscope and SEM. Bar, 50 μm. (D) Growth curves showing the quantitative proliferation of VECs in GC, Alg, and GC/Alg DN hydrogels. The bar represents the mean ± SD. (E) Growth curves showing the quantitative proliferation of BM-MSCs in GC, Alg, and GC/Alg DN hydrogels. The bar represents the mean ± SD. (F) Quantitative proliferation of the co-culture of VECs and BM-MSCs (1 : 1) in the DN hydrogel (DN-EC-BM), compared with the mono-culture of VECs (DN-EC) and BM-MSCs (DN-BM). The bar represents the mean ± SD.

EA.hy926 and BM-MSCs encapsulated in GC, Alg and DN hydrogels for 4, 7, 14, and 21 days effectively proliferated up to 21 days. It should be noticed that both EA.hy926 and BM-MSCs cultured in the DN hydrogel displayed higher cell proliferation at each time point, than cultured in GC and Alg gels (Fig. 2D and E). Interestingly, the EA.hy926 and BM-MSCs (1 : 1) co-cultured in the DN hydrogel (DN-EC-BM) presented

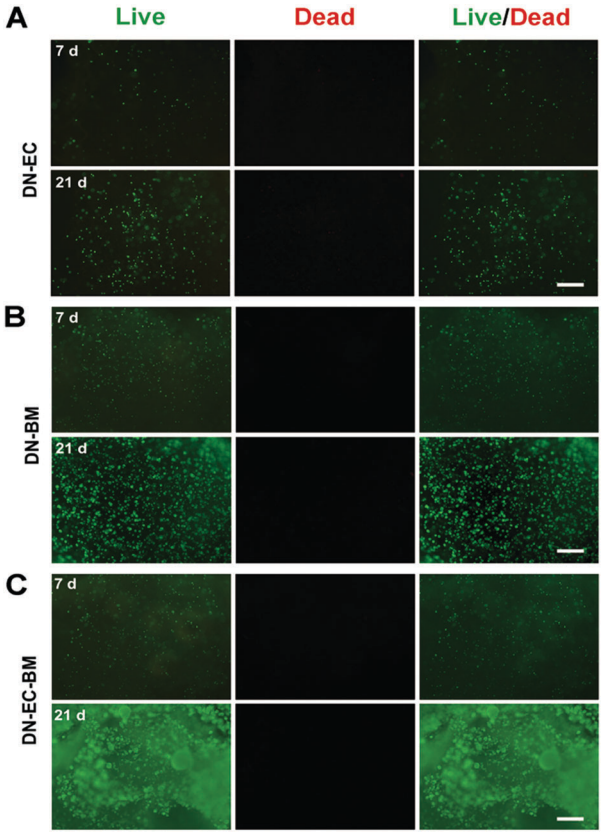

Fig. 3 (A–C) Images of Live/Dead assay staining of the mono-culture of VECs (DN-EC) and BM-MSCs (DN-BM), and the co-culture of VECs and BM-MSCs (1 : 1) in DN hydrogel (DN-EC-BM) for different indicated times (Live cells: green, Dead cells: red). Images were taken at ×40 magnification. Bar, 50 μm.

significantly increased cell proliferation than EA.hy926 and BM-MSCs mono-cultured (DN-EC and DN-BM) independently (Fig. 2F). It is speculated that there may be cross-talking between EA.hy926 and BM-MSCs encapsulating in the DN hydrogel. Live/Dead assay staining results further confirmed that the survival of EA.hy926 and BM-MSCs encapsulated in the DN hydrogel up to 21 days (Fig. 3A–C). Besides, the images also revealed that the cell population increased and the multicellular spheroids formed, with prolongation of the incubation time. It can be seen that the co-culture of EA.hy926 with BM-MSCs in the DN hydrogel could stimulate cell proliferation, appeared larger aggregation of cell spheres when comparing with ECs or BM-MSCs mono-culture group, which was consistent with the CCK-8 assay. The results of CCK-8 and Live/Dead assay demonstrated that the GC/Alg DN hydrogel as an ECM of the cells provided favorable conditions for VEC and BM-MSC encapsulation and proliferation.

Most studies linking biomaterials to cell activity have only been studied in 2D models, while a more physiologically relevant 3D culture system is essential to evaluate a bio-scaffold.[20,21] In contrast to conventional 2D monolayer cultures, spheroids are characterized by a 3D arrangement of the cells that mimic much better the *in vivo* conditions of physiological tissues.[22] Clearly, in our research, the GC/Alg DN hydrogel consisted of natural polymers (Alg and GC) which were considered well suited for 3D cell culture as they have similarities to natural ECM. The VECs and BM-MSCs encapsulated in our GC/Alg DN hydrogel 3D matrixes presented multicellular spheroids and preferred to aggregate for proliferation. The formation of cell spheroids would enhance the cell-to-cell contact and cell–matrix interaction so that the cell proliferation is promoted. In the last few years, an increasing number of studies focused on the application of spheroids as vascularization units for tissue engineering.[23] By combining endothelial cells with osteoblasts, it is possible to generate prevascularized bone or adipose spheroids, which develop a dense network of vessel-like structures during short-term cultivation.[24,25] Therefore, we further intended to explore the effects of vascularization and osteogenesis by the GC/Alg DN hydrogel encapsulating VECs and BM-MSCs co-cultured in our study.

3.3. Stimulation of angiogenic and osteogenic differentiation by the GC/Alg DN hydrogel *in vitro*

Real-Time RT-PCR was carried out to analyze angio-specific and osteo-specific gene expression from EA.hy926 and BM-MSCs cultured in the DN hydrogel at 7 or 14 days. Compared with being cultured on dishes, EA.hy926 cultured in the GC/Alg DN hydrogel (DN-EC) for 7 and 14 days showed significantly increased mRNA levels of angiogenic markers (VEGF-A, PECAM1 and vWF), and BM-MSCs cultured in the GC/Alg DN hydrogel (DN-BM) for 7 and 14 days showed significantly increased mRNA levels of osteogenic markers (Runx2, ALP and OPN) (Fig. 4A and B). Due to the increased cell proliferation of the co-cultured of VECs with BM-MSCs in the GC/Alg DN hydrogel (DN-EC-BM), it is further explored whether the co-culture could play a role in stimulating angiogenic and osteogenic differentiation. As expected, encapsulated in the DN hydrogel for 7 and 14 days, angio-specific genes of DN-EC-BM including VEGF-A, PECAM1, vWF and matrix metalloproteinase-9 (MMP-9) were upregulated compared with DN-EC, and osteo-specific genes of DN-EC-BM including Runx2, ALP and OPN were upregulated compared with the DN-BM (Fig. 4C and D). This result revealed that the co-culture of VECs with BM-MSCs could further stimulate the angiogenic and osteogenic differentiation as compared with mono-cultured cells in the DN hydrogel.

Thus, immunofluorescence staining was utilized to further validate the expression of the angio-related and osteo-related proteins at the translational level. Under the three-dimension reconstruction of LSCM, the angiogenic marker CD31 (yellow) and the osteogenic marker RUNX2 (red) enabled significantly increased expression of co-cultured group DN-EC-BM compared to that of mono-cultured group DN-EC or DN-BM at 7 and 14 days (Fig. 4E). This result corresponded to the gene analysis findings.

Histological section analysis was carried out to observe the cell morphology changes encapsulated in the DN hydrogel directly. H&E staining results exhibited that spheroids and capillary-like tubes (marked with asterisk) were formed diffusedly in DN-EC after 7 days of cultivation, and developed a dense network of capillary-like tubes along with the cultivation

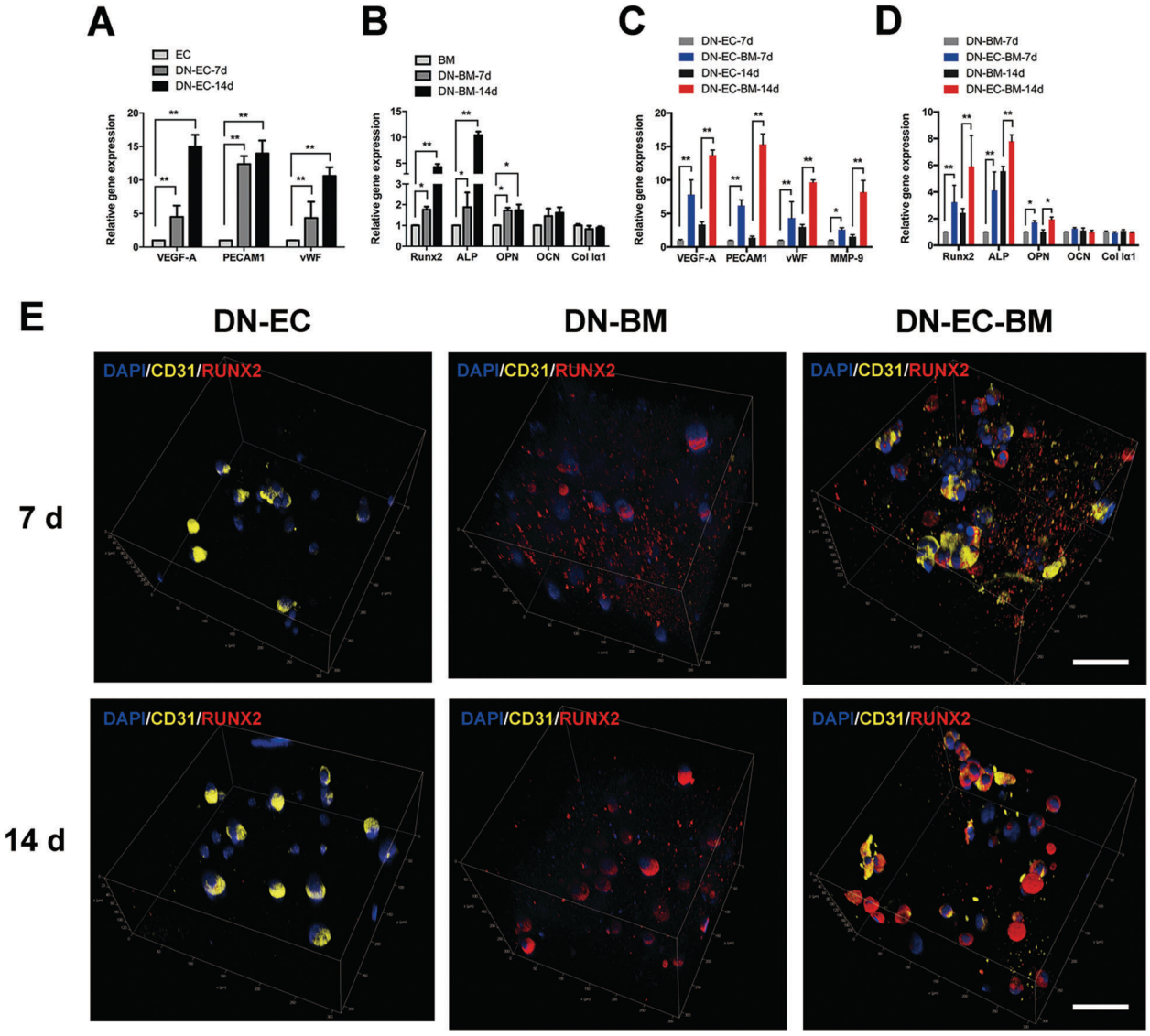

Fig. 4 Stimulation of angiogenic and osteogenic differentiation by the GC/Alg DN hydrogel *in vitro*. (A) Quantitative determination of mRNA expression of angiogenic differentiation marker genes (VEGF-A, PECAM1, and vWF) for VECs cultured in the DN hydrogel (DN-EC) for 7 d and 14 d by Real-Time RT-PCR. GAPDH was used as a control. Each bar represents the mean ± SD. $^{**}P < 0.01$. Data are shown as a fold increase in the mRNA level compared to VECs (EC). (B) Quantitative determination of mRNA expression of osteogenic differentiation marker genes (Runx2, ALP, OPN, OCN, and Col 1α1) for BM-MSCs cultured in the DN hydrogel (DN-BM) for 7 d and 14 d by Real-Time RT-PCR. GAPDH was used as a control. Each bar represents the mean ± SD. $^{*}P < 0.05$, $^{**}P < 0.01$. Data are shown as a fold increase in the mRNA level compared to BM-MSCs (BM). (C and D) Expression of angiogenic and osteogenic differentiation markers for DN-EC, DN-BM, VECs and BM-MSCs co-cultured in the DN hydrogel (DN-EC-BM) for 7 d and 14 d by Real-Time RT-PCR. GAPDH was used as a control. Each bar represents the mean ± SD. $^{*}P < 0.05$, $^{**}P < 0.01$. (E) Immunofluorescence staining of angiogenic marker CD31 (yellow) and osteogenic marker RUNX2 (red) in DN-EC, DN-BM and DN-EC-BM at 7 d and 14 d. The nuclei in both image sets were stained with DAPI (blue). Bar, 100 μm.

to 14 days (Fig. 5A). It can be seen that the generation of spheroids in DN-BM at 7 days leads to the formation of enlarged spheroids at 14 days of cultivation, and the spheroids presented calcification (marked with an arrow) (Fig. 5A). Compared with individual VECs or BM-MSCs cultured in the DN hydrogel, the co-cultured group (DN-EC-BM) appeared to form more capillary-like tubes, the spheroids grew much faster and accumulated to be calcified effectively at 14 days (Fig. 5A). As shown in Fig. 5B, von Kossa staining of DN-BM gave rise to brown stain at 14 days, indicating calcium deposition. The images of DN-EC-BM showed positive brown stain at 7 days, and exhibited dark brown and even black stain at 14 days, revealing that the co-cultured group further promoted osteogenic differentiation. In summary, the GC/Alg DN hydrogel could provide a suitable microenvironment for angiogenic and osteogenic differentiation. The co-culture of VECs and BM-MSCs in the GC/Alg DN hydrogel further stimulates the role of vascularization and osteogenesis in the gel matrix.

Recent studies suggested that the cells within spheroids have an improved differentiation potential and are more

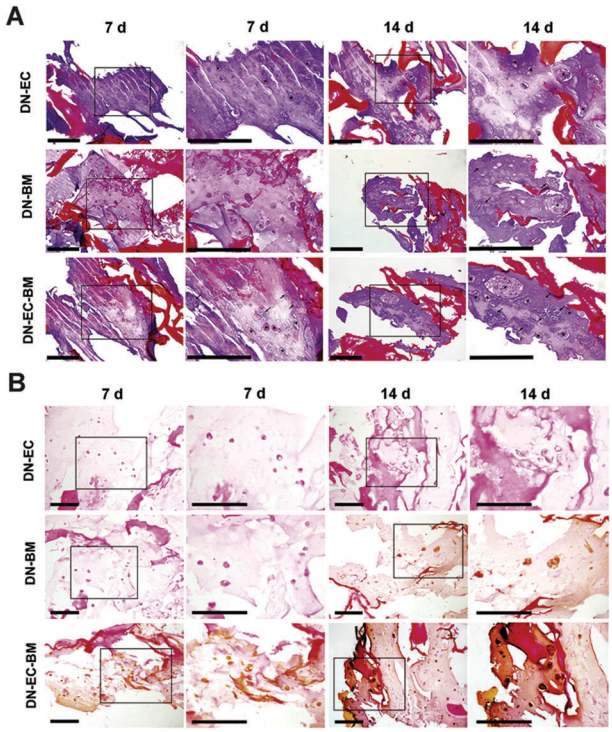

Fig. 5 (A) H&E staining and (B) von Kossa staining of histological sections for VECs cultured in the DN hydrogel (DN-EC), BM-MSCs cultured in the DN hydrogel (DN-BM), VECs and BM-MSCs co-cultured in the DN hydrogel (DN-EC-BM) at 7 d and 14 d. For each sample, images were taken at ×200 magnification (left column) and ×400 magnification (right column), respectively. Bar, 50 μm.

resistant against hypoxia and apoptotic cell death.[26,27] Moreover, they produce higher amounts of growth factors when compared to 2D cultures.[26,28] Studies indicated that ECs require an artificial ECM together with specific growth factors in the culture medium to adhere and proliferate in monoculture, most ECs cultured in 2D did not proliferate or form apparent vessel structures without a specific matrix (*e.g.*, Matrigel).[8] MSCs' osteo-differentiation based on the extent of cell–cell contact and the extent of osteo-differentiation were fairly linearly related to the extent of neighboring cells.[29] Our current data suggested that the cells effectively aggregated in the GC/Alg DN hydrogel 3D matrixes to form multicellular spheroids, increasing cell-to-cell interactions, could induce angiogenic and osteogenic differentiation to a greater extent in comparison with the 2D monolayer cell culture. These effects may be modulated by matrix mechanical properties provided by the GC/Alg DN hydrogel for cell differentiation.

For bone tissue engineering applications, biomaterial scaffolds often used for loading cells, and to enhance vascularization of tissue engineered bone, the transplantation of ECs and BMSCs together in biomaterial scaffolds has been studied, since the co-culture of ECs with BMSCs could result in the increase of angiogenic and osteogenic responses.[9,30–32] In our research, the co-culture of VECs and BM-MSCs in the GC/Alg DN hydrogel showed the strongest stimulatory effects on angiogenic and osteogenic differentiation compared with the mono-cultured VECs or BM-MSCs.

Regarding the mode of cell-to-cell communication, signaling pathways that are activated when the cells are co-cultured not only stimulate osteoblastic functions, but also endothelial functions. In addition, *via* signals that are allowed to diffuse freely in the extracellular environment and interact with the target cells through specific receptors.[8] In developing bones, VEGF-A, one of the five VEGF isoforms (VEGF-A, -B, -C, -D and -E), is expressed before blood vessels can be detected, and several studies have demonstrated its importance in bone development and in bone healing.[33,34] In co-cultured models, it has been demonstrated that VEGF has a central role in osteo-endothelial communication. It can be secreted by bone-forming cells, such as osteoblasts, osteoprogenitors or MSCs,[35] and stimulates EC proliferation, migration and formation of capillary-like structures.[35,36] In our study, VEGF-A expression was significantly increased in 3D GC/Alg DN hydrogel matrixes encapsulating co-cultured VECs and BM-MSCs. The present study indicated that cell-to-cell communication could participate in the cell migration events in combination with the release of soluble factor VEGF-A, the cross-talking between VECs and BM-MSCs may be mediated through VEGF-A and further enhanced the vascularization and osteogenic differentiation. Furthermore, our direct contact co-culture system could also regulate ECM protein (MMP-9) expression, which may play an important role in the activation of angiogenesis and bone development.

3.4. Stimulation of angiogenic differentiation by the GC/Alg DN hydrogel *in vivo*

To examine the role of vascularization and osteogenesis by the GC/Alg DN hydrogel *in vivo*, the gels encapsulated with VECs and BM-MSCs were subcutaneously implanted into nude mice, by the injection using a connected mixing syringe (Fig. 6A). The DN hydrogel without loading cells was a blank control. Fig. 6B shows the gross view of cell-loaded hydrogels that were removed from the mice at 2, 4 and 6 weeks post-implantation presented a slow degradation rate of gels *in vivo*, the residue of the implanted DN gel could be clearly found in the nude mice for up to 6 weeks. The images revealed that the DN gel caused limited immunological response of the surrounding skin, the boundary between the implants and the dermis is clear, with no damage being found in the peri-implant tissue. This result indicated the good biocompatibility of the DN hydrogel *in vivo*, which was in accordance with the above cytotoxicity experiment

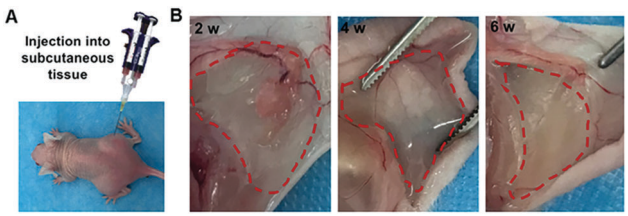

Fig. 6 Injectability of the GC/Alg DN hydrogel and *in vivo* injection. (A) Photograph of injection of the hydrogels encapsulated with VECs and BM-MSCs subcutaneously implanted into BALB/c nude. (B) The skin tissue and surrounding tissue were isolated after 2, 4 and 6 weeks of implantation, respectively.

in vitro. Due to its natural constituents, the GC/Alg DN gel exhibited negligible inflammatory response when implanted *in vivo*. It was known that chitosan derivatives have antibacteria and hemostatic potentials in implanted devices,[37] which may contribute to the reduction of the inflammation level of the GC/Alg DN gel.

H&E staining results showed that clear mature vessel-like structures were formed in co-cultures but not in mono-cultured VECs or BM-MSCs *in vivo*. The DN hydrogel without loading cells (DN) showed that the *in vivo* macrophages of nude mice assembled to phagocytose the gel, along with the process of degradation of the gel gradually. The DN gel loaded with VECs (DN-EC) or BM-MSCs (DN-BM) showed that the cells aggregated to grow and capillary-like tissues were formed in the gels at 4 and 6 weeks. The DN gel loaded with VECs and BM-MSCs (DN-EC-BM) presented showed that vessel-like tubes began to generate at 4 weeks, and further mature neovascular tubes were formed at 6 weeks (Fig. 7A). To further evaluate the *in vivo* angio-differentiation of cells encapsulated in the DN gel, the angio-specific protein CD31 was monitored by immunohistochemical (IHC) analysis at 2, 4 and 6 weeks post-implantation. IHC staining results indicated that CD31 was positively expressed in DN-EC, DN-BM and DN-EC-BM groups at 6 weeks post-implantation. Significantly, the important angiogenic marker, CD31, was much highly expressed in the DN-EC-BM group than in the other three groups at 6 weeks (Fig. 7B). Thus, all the results confirmed the hypothesis that the GC/Alg DN hydrogel provided a natural ECM niche to stimulate angiogenic differentiation of VECs and BM-MSCs, the co-culture could significantly promote the survivability and neovascularization in the gel matrix *in vivo*.

It can be seen that no effective bone matrix or mineralized bone tissues were formed up to 6 weeks during *in vivo* experiments. Recent studies have shown that the co-culture of ECs and MSCs has been used as a model of vasculogenesis and it has been investigated that MSCs can function as pericytes to promote vessel formation and maturation.[38,39] In this role, MSCs secrete specific pro-angiogenic cytokines and control the permeability of neovessels through the regulation of cell–cell adherens junctions.[40–42] In our study, it could be inferred that the undifferentiated MSCs within the spheroids may rapidly differentiate into new vessel-like tissues, and thus promote the development of new vascular structures at many different locations inside the gels in the subcutaneous environment. However, further study would be needed. It is necessary to extend the observation time of osteogenic differentiation *in vivo* in the future study. Hence, it may be reasonable to combine MSC spheroids of varying differentiation stages in tissue constructs to promote both rapid vascularization and tissue formation. These results also underlined the

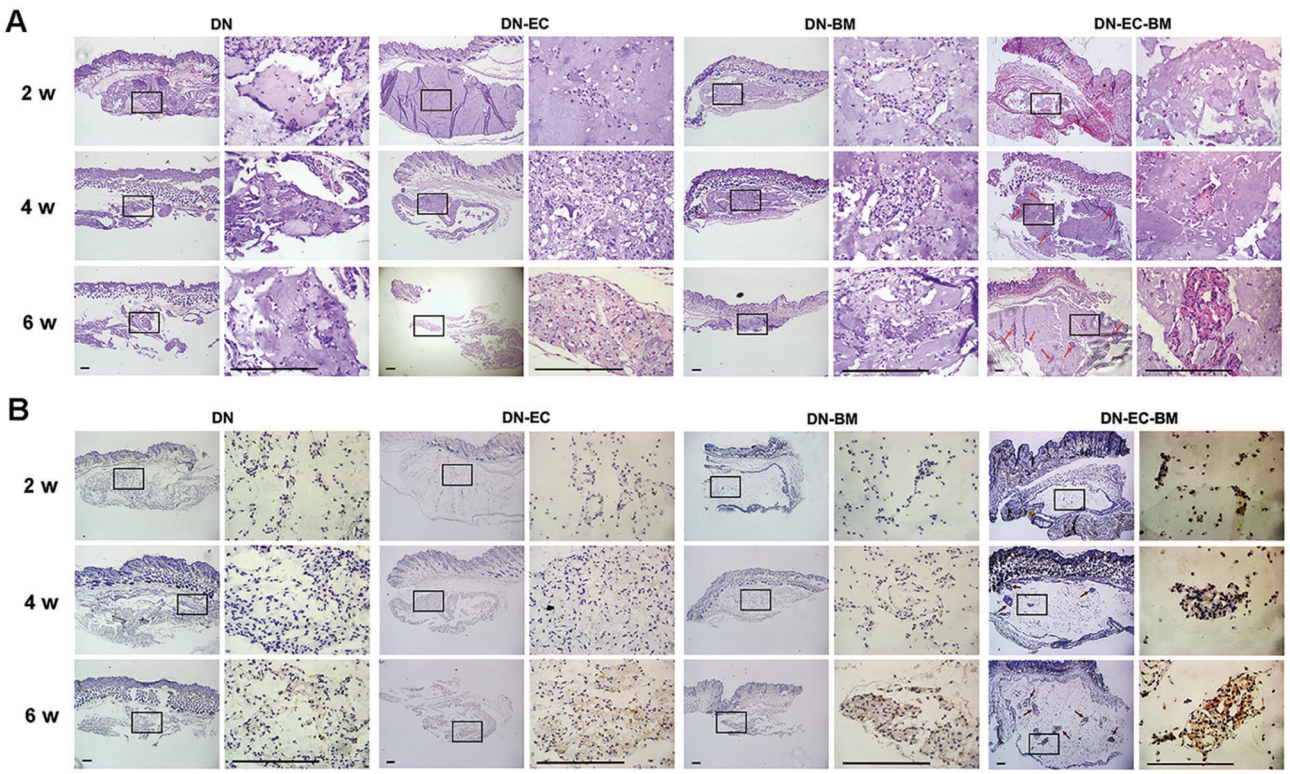

Fig. 7 Stimulation of angiogenic differentiation by the GC/Alg DN hydrogel *in vivo*. (A) H&E staining of implantation sites and surrounding tissues after the DN hydrogels encapsulated with VECs (DN-EC), BM-MSCs (DN-BM), VECs and BM-MSCs (DN-EC-BM) were injected subcutaneously harvested at 2, 4, and 6 weeks. For each sample, images were taken at ×40 magnification (left column) and ×400 magnification (right column), respectively. Bar, 100 μm. (B) Immunohistochemical (IHC) analysis of angio-specific protein CD31 in DN-EC, DN-BM and DN-EC-BM at 2, 4 and 6 weeks post-implantation. For each sample, images were taken at ×40 magnification (left column) and ×400 magnification (right column), respectively. Bar, 100 μm.

necessity to revisit the cellular or molecular factors that have already been identified as having a role in these cell-to-cell interactions.

4. Conclusions

Using a GC/Alg DN hydrogel to mimic the native ECM allows effective 3D cell encapsulation, thus providing a favorable active environment for VECs and BM-MSCs to proliferate. We demonstrate that the direct co-culture of VECs and BM-MSCs in a 3D hydrogel matrix resulted in increased vascularization and osteogenesis due to cell–cell communication both *in vitro* and *in vivo*, originating from the angiogenic and osteogenic differentiation of the stem cells. Furthermore, from the application point of view, this work also suggests that a high-performance GC/Alg DN hydrogel, with injectability as well as desirable mechanical properties, may be a beneficial biomaterial for engineering vascularized bone application.

Conflicts of interest

There are no conflicts to declare.

Acknowledgements

This work was supported by the National Natural Science Foundation of China (81771061 and 51473169).

References

1 U. Saran, S. G. Piperni and S. Chatterjee, *Arch. Biochem. Biophys.*, 2014, **561**, 109–117.
2 K. D. Hankenson, M. Dishowitz, C. Gray and M. Schenker, *Injury*, 2011, **42**, 556–561.
3 J. J. Moon and J. L. West, *Curr. Top. Med. Chem.*, 2008, **8**, 300–310.
4 W. J. Zhang, L. S. Wray, J. Rnjak-Kovacina, L. Xu, D. H. Zou, S. Y. Wang, M. L. Zhang, J. C. Dong, G. L. Li, D. L. Kaplan and X. Q. Jiang, *Biomaterials*, 2015, **56**, 68–77.
5 D. Kaigler, Z. Wang, K. Horger, D. J. Mooney and P. H. Krebsbach, *J. Bone Miner. Res.*, 2006, **21**, 735–744.
6 J. Zhou, H. Lin, T. L. Fang, X. L. Li, W. D. Dai, T. Uemura and J. Dong, *Biomaterials*, 2010, **31**, 1171–1179.
7 H. Li, K. Xue, N. Kong, K. Liu and J. Chang, *Biomaterials*, 2014, **35**, 3803–3818.
8 M. Grellier, L. Bordenave and J. Amedee, *Trends Biotechnol.*, 2009, **27**, 562–571.
9 H. Y. Li, R. Daculsi, M. Grellier, R. Bareille, C. Bourget, M. Remy and J. Amedee, *PLoS One*, 2011, **6**, e16767.
10 C. J. Kirkpatrick, S. Fuchs and R. E. Unger, *Adv. Drug Delivery Rev.*, 2011, **63**, 291–299.
11 H. Li and J. Chang, *Acta Biomater.*, 2013, **9**, 6981–6991.
12 Y. L. Li, Y. Xiao and C. S. Liu, *Chem. Rev.*, 2017, **117**, 4376–4421.
13 Y. F. Li and K. A. Kilian, *Adv. Healthcare Mater.*, 2015, **4**, 2780–2796.
14 M. P. Lutolf, P. M. Gilbert and H. M. Blau, *Nature*, 2009, **462**, 433–441.
15 D. Seliktar, *Science*, 2012, **336**, 1124–1128.
16 J. Thiele, Y. Ma, S. M. Bruekers, S. Ma and W. T. Huck, *Adv. Mater.*, 2014, **26**, 125–147.
17 Y. Yan, M. Li, D. Yang, Q. Wang, F. Liang, X. Qu, D. Qiu and Z. Yang, *Biomacromolecules*, 2017, **18**, 2128–2138.
18 F. Y. Zhu, Y. Chen, S. N. Yang, Q. Wang, F. X. Liang, X. Z. Qu and Z. B. Hu, *RSC Adv.*, 2016, **6**, 61185–61189.
19 F. Y. Zhu, C. Wang, S. Yang, Q. Wang, F. X. Liang, C. Y. Liu, D. Qiu, X. Z. Qu, Z. B. Hu and Z. Z. Yang, *J. Mater. Chem. B*, 2017, **5**, 2416–2424.
20 L. G. Griffith and M. A. Swartz, *Nat. Rev. Mol. Cell Biol.*, 2006, **7**, 211–224.
21 A. Arranja, A. G. Denkova, K. Morawska, G. Waton, S. van Vlierberghe, P. Dubruel, F. Schosseler and E. Mendes, *J. Controlled Release*, 2016, **224**, 126–135.
22 T. Andersen, P. Auk-Emblem and M. Dornish, *Microarrays*, 2015, **4**, 133–161.
23 M. W. Laschke and M. D. Menger, *Biotechnol. Adv.*, 2016, **34**, 112–121.
24 J. Rouwkema, J. De Boer and C. A. Van Blitterswijk, *Tissue Eng.*, 2006, **12**, 2685–2693.
25 R. Walser, W. Metzger, A. Gorg, T. Pohlemann, M. D. Menger and M. W. Laschke, *Eur. Cells Mater.*, 2013, **26**, 222–233.
26 S. H. Bhang, S. W. Cho, W. G. La, T. J. Lee, H. S. Yang, A. Y. Sun, S. H. Baek, J. W. Rhie and B. S. Kim, *Biomaterials*, 2011, **32**, 2734–2747.
27 H. H. Yoon, S. H. Bhang, J. Y. Shin, J. Shin and B. S. Kim, *Tissue Eng., Part A*, 2012, **18**, 1949–1956.
28 M. L. Skiles, S. Sahai, L. Rucker and J. O. Blanchette, *Tissue Eng., Part A*, 2013, **19**, 2330–2338.
29 J. Tang, R. Peng and J. D. Ding, *Biomaterials*, 2010, **31**, 2470–2476.
30 H. Y. Li, R. Daculsi, M. Grellier, R. Bareille, C. Bourget and J. Amedee, *Am. J. Physiol.: Cell Physiol.*, 2010, **299**, C422–C430.
31 R. E. Unger, A. Sartoris, K. Peters, A. Motta, C. Migliaresi, M. Kunkel, U. Bulnheim, J. Rychly and C. J. Kirkpatrick, *Biomaterials*, 2007, **28**, 3965–3976.
32 D. Kaigler, P. H. Krebsbach, E. R. West, K. Horger, Y. C. Huang and D. J. Mooney, *FASEB J.*, 2005, **19**, 665.
33 R. A. D. Carano and E. H. Filvaroff, *Drug Discovery Today*, 2003, **8**, 980–989.
34 J. Street, M. Bao, L. deGuzman, S. Bunting, F. V. Peale, N. Ferrara, H. Steinmetz, J. Hoeffel, J. L. Cleland, A. Daugherty, N. van Bruggen, H. P. Redmond, R. A. D. Carano and E. H. Filvaroff, *Proc. Natl. Acad. Sci. U. S. A.*, 2002, **99**, 9656–9661.
35 H. Mayer, H. Bertram, W. Lindenmaier, T. Korff, H. Weber and H. Weich, *J. Cell. Biochem.*, 2005, **95**, 827–839.
36 C. E. Clarkin, E. Garonna, A. A. Pitsillides and C. P. D. Weeler-Jones, *Exp. Cell Res.*, 2008, **314**, 3152–3161.
37 B. CarrenoGomez and R. Duncan, *Int. J. Pharm.*, 1997, **148**, 231–240.

38 J. M. Sorrell, M. A. Baber and A. I. Caplan, *Tissue Eng., Part A*, 2009, **15**, 1751–1761.
39 C. M. Ghajar, S. Kachgal, E. Kniazeva, H. Mori, S. V. Costes, S. C. George and A. J. Putnam, *Exp. Cell Res.*, 2010, **316**, 813–825.
40 A. I. Caplan, *Cell Stem Cell*, 2008, **3**, 229–230.
41 C. M. Ghajar, K. S. Blevins, C. C. W. Hughes, S. C. George and A. J. Putnam, *Tissue Eng.*, 2006, **12**, 2875–2888.
42 S. Pati, A. Y. Khakoo, J. Zhao, F. Jimenez, M. H. Gerber, M. Harting, J. B. Redell, R. Grill, Y. Matsuo, S. Guha, C. S. Cox, M. S. Reitz, J. B. Holcomb and P. K. Dash, *Stem Cells Dev.*, 2011, **20**, 89–101.